

PROPERTIES AND PARAMETER SELECTION FOR PHASE SYNCHRONY PROCESSING OF EEG SIGNALS

G. V. Tcheslavski and A. A. (Louis) Beex
Digital Signal Processing Research Laboratory – Systems Group
Bradley Department of Electrical and Computer Engineering, Virginia Tech
Blacksburg, Virginia, USA
gleb@vt.edu, beex@vt.edu.

ABSTRACT

The phase synchrony analysis of stochastic time series is considered with a view towards its application in EEG (electroencephalogram) processing. A Phase Synchrony Processor is proposed and its properties are examined on the basis of known signals. The observed dependence of the phase synchrony coefficient on the analysis parameters, such as the filter bandwidth and the length of the time-window, may - especially in low synchrony cases - lead to biased results. The analysis parameters can be chosen judiciously based on the results of a phase synchrony study of artificially generated signals with known phase synchrony. To illustrate the importance of the parameter choices available, a phase synchrony coefficient analysis is presented based on actual EEG.

KEY WORDS

Phase synchrony, EEG, analysis length, bandwidth.

1. Introduction

The electroencephalogram (EEG) is a weak (generally, less than 300 μ V) electrical signal obtained from electrodes placed on or under the surface of a human head. Due to the stochastic, non-Gaussian, non-linear nature of the EEG, its processing is a challenging task that has been undertaken by Fourier analysis, wavelet-based filtering, complicated linear and non-linear modeling, and matching pursuit methods [1]. In the last decade, phase-based analyses, such as phase coherence and phase synchrony, have gained particular attention as tools for processing of EEG signals [2 - 4], especially in epilepsy research [2, 3].

In this study, we concentrate on the phase synchrony analysis as proposed by Lachaux et al. [2] and Mormann et al. [3]. Their approach is based on the concept of phase synchronization of chaotic oscillators introduced by Rosenblum and colleagues [5, 6]. The latter concept seems applicable, since – from a surface EEG point of view – the human head can be modeled as a set of spatially distributed noisy oscillators operating at varying degrees of phase synchronization [7]. The phase

synchrony (coefficient) r_{lm} , also called the phase locking value, for two oscillators l and m , computed over an N_w sample long time window, is defined as follows [2 - 4]:

$$r_{lm,n} = \left| \frac{1}{N_w} \sum_{k=n-N_w+1}^n e^{-j(\varphi_{lk} - \varphi_{mk})} \right|, \quad (1)$$

where φ_{lk} and φ_{mk} denote instantaneous phase sequences for oscillators l and m respectively and n represents the time instant at which the analysis window ends. The phase synchrony coefficient takes on values between 0 (for two independent signals) and 1 (for signals that exhibit a constant difference in instantaneous phase, i.e. a signal and its time-shifted version are observed). In other words, we attempt to verify the hypothesis that a set of coupled oscillators exists that generates sinusoidal sequences of a particular frequency and that these sequences contribute to the signals recorded at different EEG electrodes. Thus, φ_{lk} and φ_{mk} must be frequency specific.

To obtain the instantaneous phase sequence, Lachaux and colleagues [2] convolved the EEG signal with the Gabor wavelet function, Allefeld and Kurths [4] applied the Morlet wavelet, and Mormann et al. [3] utilized the Hilbert transformer as an analytic signal generator. From our point of view, it is important to note that a wavelet function can be viewed as a band-pass filter. Hence, the phase sequences generated via wavelets are frequency specific. The discrete-time Hilbert transformer is a tool that can be used to produce a so-called analytic signal. Thus, to study phase synchrony in a particular band of interest, band-pass filtering is still required.

The objective of the present work is to evaluate the range of applicability of phase synchrony analysis. We use the Hilbert transformer based Analytic Signal Generator (ASG) followed by a band-pass filter, and estimate phase synchrony coefficients for artificially generated pairs of signals with known low and high synchrony. We investigate the behavior of this phase synchrony detector as a function of its parameters and compare the results to what is expected in theory, for these known signals. Finally, the importance of the parameter choices is illustrated on the basis of actual EEG records.

2. Methods

The modeled EEG time sequences are generated as sinusoids of a particular frequency, contaminated by white noise. We studied two types of signal pairs. In the high synchrony pair both signals contain noisy sinusoidal sequences of a particular frequency, i.e. the analyzed signals were highly overlapping noisy sinusoids with a constant phase shift between them (Figure 1 a). In the low synchrony pair one of the signals was normally distributed white noise (Figure 1 b).

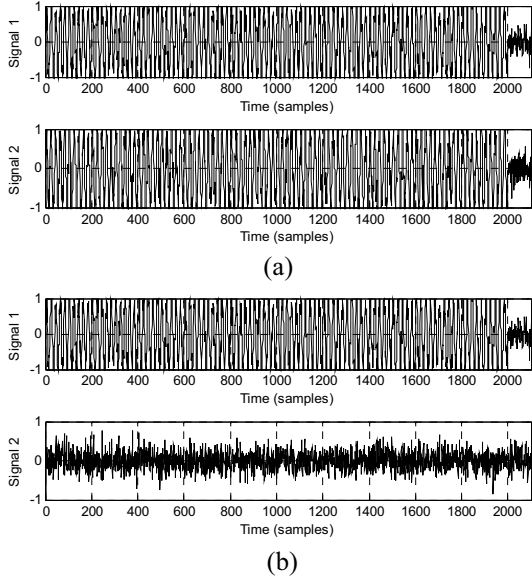


Figure 1: Signal pairs with high (a) and low (b) synchrony; $f_0 = 0.05$.

To apply phase synchrony analysis (1) to the generated pairs, we need to extract the frequency specific instantaneous phase sequences. To accomplish this, we first generate the analytic sequence corresponding to the given signal and then extract the frequency specific content for the frequency band (or EEG rhythm) of interest. These goals can be attained using the Instantaneous Phase Processor (IPP) depicted in Figure 2.

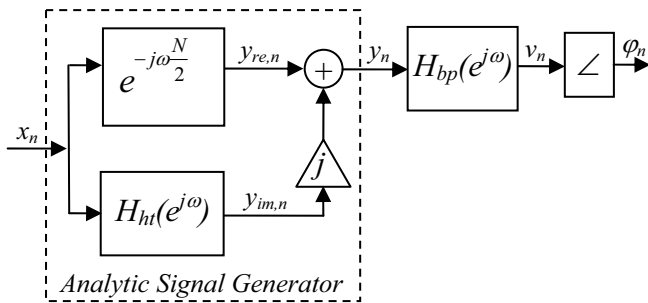


Figure 2: Frequency-specific Instantaneous Phase Processor (IPP).

The filter $H_{ht}(e^{j\omega})$ is a Kaiser-window based linear-phase FIR approximation of the ideal Hilbert transformer evaluated as follows [8]:

$$h_{ht,n} = \begin{cases} \frac{I_0 \left\{ \beta \sqrt{1 - \left[\frac{n-n_d}{n_d} \right]^2} \right\}}{I_0 \{ \beta \}} \frac{2 \sin^2 \left[\pi \frac{n-n_d}{2} \right]}{\pi (n-n_d)}, & 0 \leq n \leq N \\ 0, & \text{otherwise} \end{cases} \quad (2)$$

where I_0 represents the zeroth-order modified Bessel function of the first kind, $N+1$ is the specified length of the Hilbert transformer FIR approximation ($N+1 = 51$ was used in this study), $n_d = N/2$, and β , chosen as 2.629, is a parameter that controls smoothness of spectral transition. N and β were selected to achieve a peak approximation error of less than 0.018 (-35 dB) in the fractional frequency band from 0.04 to 0.46.

The real part of the analytic signal y_n is the real input signal delayed by $N/2$ samples (25 in our case). The band-pass filter $H_{bp}(e^{j\omega})$ was implemented as an equiripple FIR filter with adjustable center frequency f_c and adjustable bandwidth B . The length of the filter was estimated based on pass-band and stop-band ripples of 0.01, a transition band of 0.05 in fractional frequency, and the given bandwidth B .

To process a pair of signals according to (1), the Phase Synchrony Processor (PSP), depicted in Figure 3, is employed.

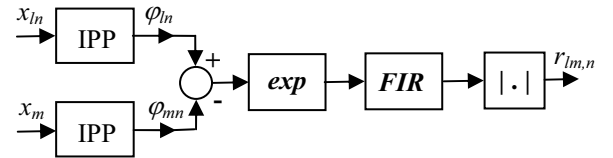


Figure 3: Phase Synchrony Processor (PSP).

The instantaneous phase sequences associated with the two input signals x_{ln} and x_{mn} are generated by two identical IPPs, subtracted, and that difference produces the corresponding unit magnitude phasor. The resulting sequence of phasors is filtered by the FIR filter performing time averaging over an N_w sample-long window, which here is chosen to be rectangular. Finally, the absolute value of the result of this filtering is $r_{lm,n}$, a sequence of phase synchrony coefficients.

The advantage of the PSP - compared to wavelet filtering - is parameter flexibility since the length of the analysis time window, the center frequency, and the filter bandwidth can be adjusted independently.

3. Results

The phase synchrony processor (Figure 3) was implemented in Matlab and numerical experiments with

artificially generated signal pairs, generated as described in Section 2 for various signal lengths, were performed.

3.1. Expected Value of Phase Synchrony

For the high synchrony signal pair (Figure 1a), the two input signals are at the same frequency. The phase difference $\Delta\varphi_k = \varphi_{lk} - \varphi_{mk} = \varphi_0$ is constant and the phase synchrony is therefore, in theory,

$$r_{lm,n} = \left| \frac{1}{N_w} \sum_{k=n-N_w+1}^n e^{-j\varphi_0} \right| = \frac{1}{N_w} |N_w \cdot e^{-j\varphi_0}| \equiv 1. \quad (3)$$

Evaluating the expected value of phase synchrony for the low synchrony pair, we have assumed for simplicity that $n = N_w$ and $\Delta\varphi_k = \varphi_{lk} - \varphi_{mk}$ in (1), so that

$$\begin{aligned} r_{lm,N_w} &= \left| \frac{1}{N_w} \sum_{k=1}^{N_w} e^{-j\Delta\varphi_k} \right| = \frac{1}{N_w} \left| \sum_{k=1}^{N_w} \cos \Delta\varphi_k - j \sum_{k=1}^{N_w} \sin \Delta\varphi_k \right| \\ &= \frac{1}{N_w} \sqrt{\left(\sum_{k=1}^{N_w} \cos \Delta\varphi_k \right)^2 + \left(\sum_{k=1}^{N_w} \sin \Delta\varphi_k \right)^2} \\ &= \frac{1}{N_w} \sqrt{N_w + 2 \sum_{i=1}^{N_w-1} \sum_{k=i+1}^{N_w} \cos(\Delta\varphi_i - \Delta\varphi_k)} \end{aligned} \quad (4)$$

where the phase differences $\Delta\varphi_i$ and $\Delta\varphi_k$ are assumed to be uniformly distributed over $[-\pi, \pi]$.

By expanding (4) and substituting

$$\xi_{N_w} = \frac{1}{N_w^2} \sum_{i=1}^{N_w-1} \sum_{k=i+1}^{N_w} \cos(\Delta\varphi_i - \Delta\varphi_k), \quad (5)$$

the phase synchrony in (4) can be rewritten as

$$r_{lm,N_w} = \sqrt{\frac{1}{N_w} + 2\xi_{N_w}}. \quad (6)$$

Numerical experiments show that the term in (5) is represented well by a shifted exponential random variable with distribution

$$f_{\xi}(\xi) = N_w e^{-N_w \left(\xi + \frac{1}{2N_w} \right)}, \quad \xi \geq -\frac{1}{2N_w}. \quad (7)$$

The expected value of phase synchrony for the low synchrony signal pair is now found as follows:

$$E\{r\} = \int_0^1 r \cdot f_{\xi}(\xi) \cdot d\xi = N_w \int_0^1 \sqrt{\frac{1}{N_w} + 2\xi} \cdot e^{-N_w \left(\xi + \frac{1}{2N_w} \right)} d\xi. \quad (8)$$

These expected values of phase synchrony, as obtained by numerical evaluation of (8) for different lengths of analysis window, are shown in Figure 4. The 100 trial averages of the numerical simulation of (4) with uniformly distributed $\Delta\varphi_k$ are shown in Figure 4 also.

Figure 4 suggests that the average phase synchrony value for the low synchrony pair never reaches zero for finite N_w , and that this value is higher for shorter analysis windows.

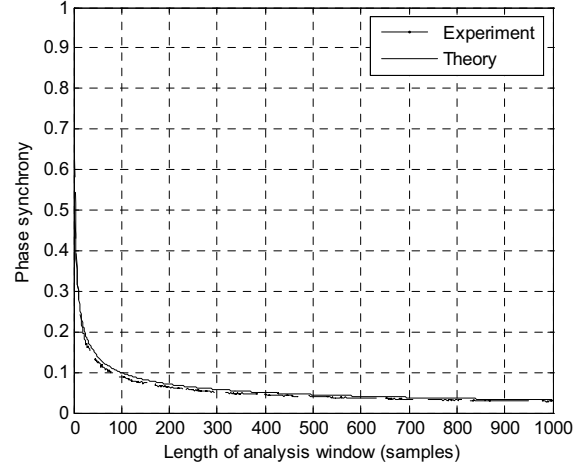


Figure 4: Expected value of phase synchrony for the low synchrony pair and its experimental approximation.

We note that the theoretically expected value of phase synchrony for the low synchrony case can be approximated according to Pikovsky et al. [6] as:

$$E\{r\} \approx \frac{1}{\sqrt{N_w}}. \quad (9)$$

We conclude that the effect of shortening the finite observation length is an increased bias in phase synchrony for zero synchrony signal pairs.

3.2. Phase Synchrony Analysis of Simulated Signals

The inputs of the PSP were either the high synchrony pair (Figure 1a) or the low synchrony pair (Figure 1b). In both cases, the sinusoidal signals were contaminated by white Gaussian noise with SNR of 10 dB. For the channel containing the sinusoidal signal, Figure 5 depicts the instantaneous phase sequences of the signals y_n and v_n (Figure 2), that is, before and after narrow-band filtering (center frequency was 0.05; bandwidth was 0.005 and the transition band was 0.005 in fractional frequency; ripples were 0.01; the filter length N_{bp} was 489). The vertical line in Figure 5a – at sample 2,000 – represents the end of the sinusoid. Time delays due to filtering were accounted for by discarding the first $\left\lfloor \frac{N_{bp}}{2} \right\rfloor$ time samples.

We observe that the filtering operation has little effect on the phase of the sinusoidal signal (to the left of the vertical line in Figure 5a) since the center frequency of the filter and the frequency of the sinusoid are the same. On the other hand, the phase of the filtered noise remains nearly linear (Figure 5a). Even after a considerable time, the phase sequence of the filtered noise still exhibits approximately linear behavior (Figure 5b).

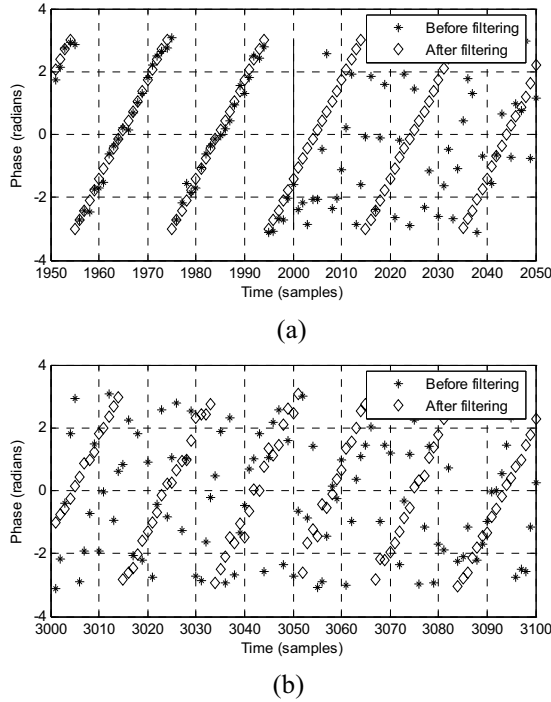


Figure 5: Instantaneous phase signals before and after narrow-band ($B = 0.005$) filtering, for time intervals 1950-2050 (a) and 3000-3100 (b).

This effect leads to a nearly constant phase difference between two filtered random sequences (Figure 6a). Phase relations are more complicated when processing actual time series, such as an EEG, but the general influence of the parameters is seen to be similar (Figure 6b).

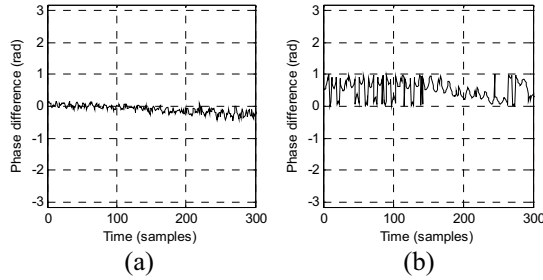


Figure 6: Phase differences for the low synchrony pair (a) and for a real EEG signal pair (b).

Both results were obtained for a bandwidth of 0.005 and exhibit little variation in the phase differences. The latter indicates high synchrony, which for the case of Figure 6a is known to be incorrect.

We next consider the low synchrony signal pair generated similarly to the one shown in Figure 1b, except the length of the signals was varying. For such signal pairs, the value of phase synchrony is expected to be close to zero. The theoretical limit for low synchrony pairs has been evaluated in the previous section. The phase synchrony estimated by the PSP for the low synchrony pair is averaged over 100 trials. The Parks-McClellan FIR filter with fractional center frequency of 0.05, bandwidth of 0.02, transition band of 0.005 in fractional frequency,

and pass-band and stop-band ripples of 0.01 (filter length of 489) was used. The results are presented in Figure 7, and contrasted with the theoretical expectation as evaluated in Section 3.1.

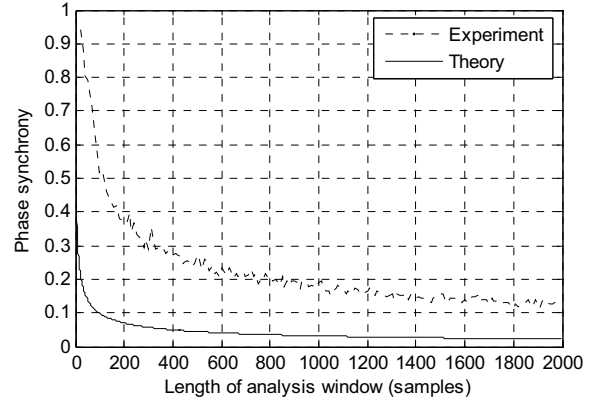


Figure 7: Low synchrony pair phase synchrony: theoretical expectation and averaged PSP output (100 trials); $B = 0.02$.

Figures 4 and 7 display the same theoretical result, i.e. the expected phase synchrony. However, the experimental result in Figure 7 is based on analysis of the PSP output, which is affected by band-pass filtering, while Figure 4 shows the result of simulation of (1) as discussed in Section 3.1. We conclude from Figure 7 that the filtering operation introduces an additional bias for low synchrony signal pairs. This is consistent with the earlier observation that band-pass filtered noise produces relatively linear instantaneous phase and this violates the uniformly distributed phase assumption used to derive the theoretical result.

The result of the Monte Carlo experiment conducted on low synchrony pairs for varying bandwidths and lengths of analysis window is shown in Figure 8. Each value was obtained by averaging the results for 100 repetitions of signal pairs and statistically independent noise with SNR = 10 dB. The fractional center frequency of the band-pass filter was chosen as 0.05, which corresponds to the upper bound of the α -rhythm for a 256 Hz sampling frequency. The length of the sinusoidal signal exceeded the length of the analysis window, so as to avoid any transient effects. The phase synchrony coefficients along the contours are equal to the indicated values.

We observe in Figure 8 that the length of the analysis time window, denoted as N_w in (1), has a major effect on phase synchrony. Namely, the shorter the window is, the higher the phase synchrony coefficient bias. Consequently, the shorter the window is, the higher the likelihood of error for the low synchrony pair.

In addition to the length of analysis window, the bandwidth of the filter greatly influences the values of phase synchrony. We observe that the narrower the bandwidth is, the higher the expected phase synchrony

value, and therefore the higher the likelihood of bias error for the low synchrony pair.

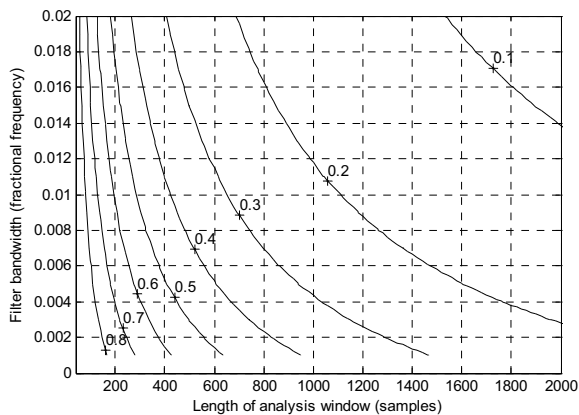


Figure 8: Average phase synchrony for low synchrony pair for different filter bandwidths and analysis window lengths.

We also observe that the average phase synchrony decreases faster with an increase of the analysis window length than with a comparable increase in filter bandwidth. We conclude from this observation that the choice of the length the analysis window is more influential than the selection of the filter bandwidth.

The same values of average phase synchrony were observed – at a given filter bandwidth and length of analysis window – for different choices of center frequency of the band-pass filter.

The corresponding results for high synchrony pairs showed minimal dependence on bandwidth and analysis window length. The phase synchrony exceeded 0.99 for the entire range of filter parameters used for Figure 8.

3.3. Phase Synchrony Analysis of EEG

For illustrative purposes, we next present an example of phase synchrony evaluated for an actual EEG record collected according to International 10-20 electrode placing from a healthy subject performing a reading task. The EEG signal was sampled at the rate of 256 Hz and then processed according to (1) using band-pass filters with center frequency $f_0 = 10$ Hz and bandwidth of either 0.02 or 0.001 in fractional frequency, i.e. 4 Hz or 0.256 Hz respectively (all or part of α -rhythm). The length of the analysis window was 400 samples. The results for all 19 electrode pairs for one particular time interval are shown in Figure 9. Each square in Figure 10 corresponds to a phase synchrony coefficient evaluated for the particular pair of electrodes. Note that the diagonal elements are one since auto-synchrony of a signal pair is always identical to one.

As seen in Figure 9, a narrow bandwidth (lower-right triangle) tends to produce high values of phase synchrony coefficients. In our modeled results we observed that this can happen regardless of whether phase synchrony is actually low or high.

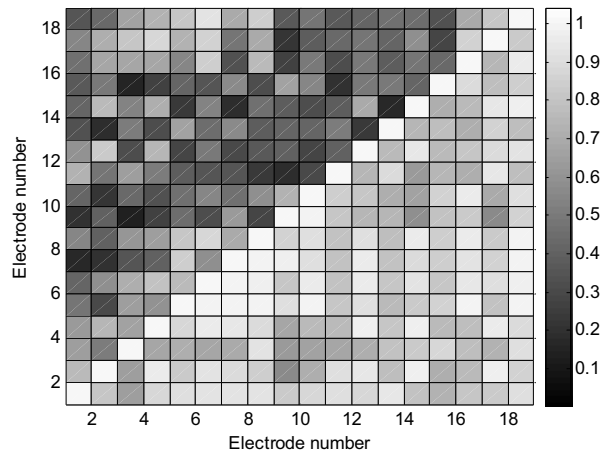


Figure 9: Phase synchrony between different pairs of EEG electrodes; $f_0 = 10$ Hz (0.039 in fractional frequency), $N_w = 400$ samples, bandwidth 0.02 (upper-left triangle) and 0.001 (lower-right triangle).

These results suggest that to be able to discriminate between low and high synchrony, sufficiently long analysis windows and band-pass filters with sufficiently broad bandwidth be used. For instance, studying the EEG α -rhythm (8 – 12 Hz), the center frequency of the band-pass filter would be 10 Hz and the bandwidth 0.02. Thus, as seen in Figure 8, to obtain a phase synchrony coefficient of approximately 0.2 (on average) for a low synchrony signal pair, the length of the analysis window must be almost 700 samples. Assuming a sampling rate of 256 Hz, we see that EEG records of almost 3 seconds need to be processed. If less discrimination is acceptable, and a phase synchrony coefficient under 0.4 (on average) is used, the analysis window needs to be over 250 samples long (approximately 1 second).

An other possibility for decreasing the observation time – while maintaining a low phase synchrony bias – is to use a higher sampling rate. For instance, by doubling the sampling frequency from 256 Hz to 512 Hz and keeping the analysis window length the same, the actual observation time will be halved. This increase in the sampling rate halves the center frequency and the bandwidth of the band-pass filter (in terms of fractional frequency). The latter increases the phase synchrony bias from 0.2 to 0.28 for an analysis length of 700, while keeping the absolute bandwidth the same (i.e. we’re looking at exactly the same rhythm). To return to the earlier phase synchrony bias of 0.2, either the filter bandwidth must be increased accordingly (which we’re not interested in), or the length of the analysis window must be increased. The latter requires an increase in analysis window length to 1100. Note that the corresponding duration of the EEG record is 2 seconds, which is less than doubled.

The example of phase synchrony evaluation for a real EEG record suggests that shorter term (lower N_w) phase

synchrony evaluation is subject to increasingly larger errors in discriminating between high and low synchrony.

This study shows that the phase synchrony analysis of EEG records tends to produce high results – which may be inadequate – while processing short EEG sequences or when narrow-band filtering is applied.

4. Conclusion

The choice of phase synchrony processor parameters is very important for reliable phase synchrony studies. The results presented here suggest using broad-band filters and long analysis windows when possible. Application to EEG signals indicates that long term synchrony can be evaluated adequately, provided processing parameters are chosen judiciously.

5. References

[1] K.J. Blinowska and P.J. Durka, “Unbiased high resolution method of EEG analysis in time-frequency,” *Acta Neurobiology*, vol. 61, pp. 157-174, 2001.

[2] J.-P. Lachaux, E. Rodrigues, J. Martinerie, and F.J. Varela, “Measuring phase synchrony in brain signals,” *Human Brain Mapping*, #8, pp. 194-208, 1999.

[3] F. Mormann, K. Lehnertz, P. David, C.E. Elger, “Mean phase coherence as a measure for phase synchronization and its application to the EEG of epilepsy patients,” *Physica*, vol. D, #144, pp. 358-369, 2000.

[4] C. Allefeld and J. Kurths, “Multivariate phase synchronization analysis of EEG data,” *IEICE Transactions Fundamentals*, vol. E86-A, #9 September, 2003, pp. 2218-2221, 2003.

[5] M.G. Rosenblum, A.S. Pikovsky, and J. Kurths, “Phase synchronization of chaotic oscillators,” *Physical Review Letters*, vol. 76, #11, March 1996, pp. 1804-1807, 1996.

[6] Pikovsky A., Rosenblum M., and Kurths J.: *Synchronization: a universal concept in nonlinear sciences*. The Cambridge nonlinear science series, Cambridge, 2001.

[7] R.M. Leahy, J.C. Mosher, M.E. Spencer, M.X. Huang, and J. Lewine, “A study of dipole localization accuracy for MEG and EEG using a human skull phantom”, *Los Alamos Technical Report: LA-UR-98-1442*, March 1998.

[8] Oppenheim A.V., Schafer R.W.: *Discrete-time signal processing*. Prentice Hall signal processing series, New Jersey, 1989.